MolecularMedicine

Interrelationship between Changes in the Amyloid β 42/40 Ratio and Presenilin 1 Conformation

Katarzyna Marta Zoltowska, Masato Maesako, and Oksana Berezovska

MassGeneral Institute for Neurodegenerative Disease, Massachusetts General Hospital, Harvard Medical School, Department of Neurology, Charlestown, Massachusetts, United States of America

The ratio of the longer (Aβ42/Aβ43) to shorter (Aβ40) species is a critical factor determining amyloid fibril formation, neurotoxicity and progression of the amyloid pathology in Alzheimer's disease. The relative levels of the different Aβ species are affected by activity and conformation of the γ-secretase complex catalytic component presenilin 1 (PS1). The enzyme exists in a dynamic equilibrium of the conformational states, with so-called "close" conformation associated with the shift of the γ-secretase cleavage toward the production of longer, neurotoxic Aβ species. In the current study, fluorescence lifetime imaging microscopy, spectral Förster resonance energy transfer, calcium imaging and cytotoxicity assays were utilized to explore a reciprocal link between the Aβ42 and Aβ40 peptides present at various ratios and PS1 conformation in primary neurons. We report that exposure to Aβ peptides at a relatively high ratio of Aβ42/40 causes conformational change within the PS1 subdomain architecture toward the pathogenic "closed" state. Mechanistically, the Aβ42/40 peptides present at the relatively high ratio increase intracellular calcium levels, which were shown to trigger pathogenic PS1 conformation. This indicates that there is a reciprocal cross-talk between the extracellular Aβ peptides and PS1 conformation within a neuron, with Aβ40 showing some protective effect. The pathogenic shift within the PS1 domain architecture may further shift the production of Aβ peptides toward the longer, neurotoxic Aβ species. These findings link elevated calcium, Aβ42 and PS1/γ-secretase conformation, and offer possible mechanistic explanation of the impending exacerbation of the amyloid pathology.

Online address: http://www.molmed.org
doi: 10.2119/molmed.2016.00127

INTRODUCTION

Alzheimer's disease (AD) is a neurodegenerative disorder characterized by accumulation of the extracellular amyloid β (Aβ) aggregates in the brain, as one of the major pathological hallmarks of the disease (1,2). The presenilin 1 (PS1)/γ-secretase cleavage releasing Aβ can occur at several positions within the transmembrane region of APP, resulting in production of a mixture of peptides varying in their length and aggregation properties (3–5). The majority of the peptides produced constitute the Aβ40 species. However, greater emphasis has been placed on the longer Aβ42/43 peptides that are detected at approximately 10-fold lower levels than Aβ40. The longer Aβ peptides have strong neurotoxicity and intrinsic self-assembly properties, promoting their accumulation in the extracellular amyloid plaques (6,7).

Importantly, the vast majority of mutations in APP and PS1 shift the spectrum of Aβ peptides toward the longer species (http://www.alzforum.org/mutations) (8). A small elevation in the Aβ42/40 ratio increases Aβ peptide's aggregation properties, induces neurotoxicity and alters synaptic activity in primary neurons (9). On the other hand, it was suggested that Aβ40 might serve as a protective factor in AD progression, mediating the inhibition of Aβ42 fibrillogenesis (10). Collectively, these data suggest that elevated Aβ42/40 ratio is linked to AD pathogenesis and could be targeted therapeutically.

The elevation of the Aβ42/40 ratio in the pathogenic condition might be attributed to the conformational shift in PS1, a catalytic subunit of the γ-secretase complex. The mature form of the enzyme can adopt different conformational states, as determined by the single particle electron microscopy and fluorescence lifetime imaging (FLIM) (11,12). The close PS1 domain proximity, as it is observed in the familial AD

Address correspondence to *Oksana Berezovska . MassGeneral Institute for Neurodegenerative Disease, Massachusetts General Hospital, Harvard Medical School, Department of Neurology, 114 16th Street, Charlestown, MA 02129. Phone: 1-617-726-7478; Fax: 1-617-724-1480; E-mail: oberezovska@partners.org*
Submitted May 10, 2016; Accepted for publication July 5, 2016; Published Online (www.molmed.org) July 5, 2016.

Feinstein Institute for Medical Research
Northwell Health™

mutant PS1, favors γ-secretase cleavage site(s) on APP, producing longer Aβ species (13). Hence, we refer to this state as "closed," pathogenic PS1 conformation. Importantly, pathogenic PS1 conformation, elevated production of the longer, fibrillogenic Aβ species and consequent increase in the Aβ42/40 ratio, leading to gradual amyloid deposition, occur during aging, and in sporadic AD brains (14–16). Of note, the occurence of PS1 conformational change correlates with the proximity to Aβ plaques (15). On the other hand, compounds that allosterically modulate PS1 by shifting it toward the "open" conformation consequently shift the spectra of Aβ species toward the shorter peptides (11,17,18). This suggests that PS1 conformational change is upstream of the various amyloid β specie production. However, it remains unclear whether there is a reciprocal cross-talk between Aβ and PS1/γ-secretase conformational changes.

This study investigates a mechanistic link between the high Aβ42/40 ratio and PS1 conformation. We found that a mixture of Aβ40 and Aβ42 peptides at the relatively high Aβ42/40 ratio can reciprocally modulate PS1 conformation by shifting it toward the pathogenic state. We propose that this is mediated by increased intracellular calcium levels. Such conformational shift, in turn, results in a greater production of the Aβ42 relative to Aβ40, and may promote further rapid cell-autonomous and noncell-autonomous spread of the amyloid pathology within the brain.

MATERIALS AND METHODS

Plasmids

Adeno-associated viral (AAV) vector plasmid encoding presenilin 1 (PS1) with the green fluorescent protein (GFP) fused to the N-terminus and the red fluorescent protein (RFP) inserted in the loop domain, under hSyn1 promoter, was used as a reporter of the PS1 conformation. The plasmid was packaged in AAV serotype 8 capsid at University of Pennsylvania Vector Core.

Primary Neuronal Cultures

Mixed cortical primary neuronal cultures were obtained from cerebral cortex of CD1 wild type mouse embryos at gestation d 16–18. The dissected tissue was dissociated using Papain Dissociation Kit (Worthington Biochemical Corporation), the neurons were plated on poly-D-lysine coated dishes and cultured in Neurobasal Medium supplemented with 10% fetal bovine serum, 2% B27, 1% penicillin/streptomycin and 1% Glutamax (ThermoScientific) in 37°C, 5% CO_2 incubator. When necessary, the neurons were infected at 5 d *in vitro* (DIV) with AAV viruses by addition of the respective AAV stocks into culture media, and 6 d incubation prior to the analysis.

All experiments involving animals were performed under national (United States National Institutes of Health) and institutional (Massachusetts General Hospital Subcommittee for Research Animal Care) approved guidelines.

Amyloid β Preparation and Treatment

The Aβ peptides were prepared as described previously (9,19). Briefly, Aβ42 and Aβ40 peptides (Peptide Institute) dissolved at 1 mg/mL concentration in hexafluoroisopropanol (HFIP), were mixed in molar ratio of 1:9, 3:7, 4:6, 1:0, 4:0 and 10:0, respectively. HFIP was evaporated and the peptides were resuspended in PBS/2% DMSO to the final concentration of 22 μmol/L. Then the samples were filtered using 0.2 μm Whatman Polyethersulfone (PES) Filter Puradiscs (GE Healthcare Bio-Sciences). The samples were kept on ice with the lag time maximum of 15 min. For the treatment of primary neurons, the peptides were diluted in Neurobasal Medium to 1 μmol/L or 10 nmol/L final concentration and the incubation was continued for 2 h at 37°C.

Immunocytochemistry

Neurons were fixed with 4% paraformaldehyde in phosphate-buffered saline (PBS), permeabilized with 0.1% Triton-X, and the nonspecific binding of antibodies was blocked by 1 h incubation with 1.5% normal donkey serum (NDS) (Jackson ImmunoResearch Labs). Anti-PS1 N-terminus (Abcam) and anti-PS1 loop domain (Abcam) primary antibodies were applied overnight at 4°C. Corresponding Alexa Fluor 488- and Cy3-conjugated secondary antibodies were used for detection. The slides were mounted using Vectashield mounting medium (Vector Laboratories Inc.).

Fluorescence Lifetime Imaging Microscopy (FLIM)

The relative proximity between fluorescently labeled N-terminus and the cytoplasmic loop domain between the transmembrane helices 6 and 7 of the endogenous PS1 was determined by previously validated FLIM assay for PS1 conformation (11). Briefly, pulsing Chameleon Ti:Sapphire laser (Coherent Inc.) was used to excite Alexa Fluor 488 donor fluorophore (two-photon excitation at 780-nm wavelength). The lifetimes of the donor fluorophore were recorded using a high-speed photomultiplier tube (MCP R3809; Hamamatsu) and a fast time-correlated single-photon counting acquisition board (SPC-830; Becker & Hickl). The baseline lifetime of the donor fluorophore (Alexa Fluor 488) in the absence of the acceptor (Cy3) was determined as the Förster resonance energy transfer (FRET) negative control (τ1). The presence of acceptor fluorophore < 10 nm from the donor results in FRET and a characteristic shortening of the donor fluorophore lifetime (τ2). The degree of the donor lifetime shortening correlates with the relative proximity between the fluorophores. The percent FRET efficiency (E_{FRET}%) is calculated as follow: $E_{FRET}\% = (\tau1-\tau2)/\tau1*100\%$. The images were acquired using Zeiss LSM510 confocal microscope with ZEN 2009 software equipped with Zeiss 63x/1.4 Oil DIC objective. The data were analyzed using SPC Image software (Becker & Hickl).

Spectral FRET

Spectral FRET assay was performed as described previously (20). Briefly, the GFP was excited using the Argon laser

at 488 nm and emitted fluorescence was detected at 513 ± 10.57 nm (GFP) and 598 ± 10.57 nm (RFP) spectral bandwidth of the Metadector in the Zeiss LSM510 confocal microscope equipped with Zeiss 25x/0.8 Corr DIC objective, with ZEN 2009 software. Fluorescence intensity of individual neurons was measured using ImageJ 1.46c software. The ratio of the 598 nm to 513 nm fluorescence intensity was used as a readout of the FRET efficiency, that is, the relative proximity between the GFP- and RFP-labeling respective PS1 domains.

Calcium Imaging

Calcium influx was induced by the application of 50 mmol/L KCl or 5 μmol/L calcium ionophore A2317 (Sigma Aldrich). The intracellular calcium levels were determined using ratiometric dye Indo-1, as described previously (21). Briefly, Indo-1/AM (ThermoScientific) was dissolved with 20% pluronic F-127 (ThermoScientific) in DMSO and added to the culture dishes at a final concentration of 1 μmol/L Indo-1/AM and 0.02% pluronic F-27 for 45 min. Cells were imaged with ZEN 2009 software using Zeiss LSM510 inverted confocal microscope equipped with Zeiss 25x/0.8 Corr DIC objective. The Chameleon Ti:Sapphire laser was used at 750-nm two-photon excitation, and the emitted light was discriminated into two channels with interference filters corresponding to 390 nm, 65-nm bandpass and 495 nm, 20-nm bandpass (Chroma Technology). The data was analyzed using ImageJ 1.46c software.

Alternatively, changes in the intracellular calcium level were determined using Oregon Green BAPTA-1/AM (ThermoScientific). The neurons were loaded with 5 μmol/L Oregon Green BAPTA-1/AM by 30-min incubation in Ca^{2+}/Mg^{2+} Hank's Balanced Salt Solution (ThermoScientific). The dye was washed off and the cells were imaged with ZEN 2009 software using Zeiss LSM510 inverted confocal microscope equipped with Zeiss 25x/0.8 Corr DIC objective.

Enzyme-Linked Immunosorbent Assay (ELISA)

The abundance of the Aβ oligomers that have at least two intact N-termini in the Aβ preparations was determined using amyloid-β oligomers 82E1-specific ELISA (IBL America) according the manufacturer's protocol.

Dot Blot

Aβ oligomers were detected using the dot blot method. Briefly, the Aβ preparations were applied on the nitrocellulose membrane (GE Healthcare Lifesciences). The nonspecific binding was blocked using Odyssey Blocking Buffer (LI-COR) and the membranes were probed with the anti-amyloid oligomers A11 antibody (Abcam) and a corresponding secondary antibody (LI-COR). The signal was developed using the digital imaging system LI-COR Odyssey scanner.

Cytotoxicity Assay

The cytotoxicity was determined using a cytotoxicity detection kit (Sigma-Aldrich) according to the manufacturer's recommendation. Briefly, 50 μL of the conditioned medium were mixed with 50 μL of the reaction mixture and incubated in dark for 20 min at room temperature. The absorbance at 490 nm was read using a Wallac plate reader (PerkinElmer).

Statistical Analysis

Statistical significance was calculated with GraphPad Prism 5 software using a two-tailed unpaired Student *t* test or Pearson's X-square test. p value of < 0.05 was a predetermined threshold for statistical significance.

All supplementary materials are available online at www.molmed.org.

RESULTS

Aβ42/40 Ratio Modulates PS1 Conformation

Fluorescence lifetime imaging microscopy (FLIM), combined with the immunohistochemical analysis of human sporadic AD (sAD) brains revealed that PS1 exists in the "closed" pathogenic state in neurons proximal to the amyloid deposits (15). To determine whether an increase in the Aβ42 and/or the Aβ42/40 ratio can in turn modulate PS1 subdomain arrangement, we incubated primary neurons with Aβ mixtures containing Aβ42 to Aβ40 in the following ratios: 1:9; 3:7; 4:6; 10:0. The cells were treated for 2 h with the total Aβ at 1 μmol/L final concentration. The applied Aβ peptide preparations were characterized by oligomeric Aβ enzyme-linked immunosorbent assay (ELISA) and dot blot with oligomeric Aβ specific antibody (Figure 1). As expected, the increase in the Aβ42 amount relative to Aβ40 resulted in the greater abundance of the oligomeric Aβ species. Interestingly, the relatively small change in the Aβ42/40 ratio from 3:7 to 4:6 resulted in a profound increase in the fibrillogenic properties of the Aβ peptides.

Following the treatment, endogenous PS1 conformation was analyzed by measuring relative proximity between the fluorophores labeling the PS1 N-terminus and the PS1 loop domain using antibody-based FLIM. There was no significant difference in the PS1 conformation between vehicle-treated neurons and those treated with the Aβ42/40 at the 1:9 and 3:7 ratios. However, characteristic shortening of the donor fluorophore lifetime, indicative of the increased FRET efficiency, was detected when the cells were treated with the Aβ42/40 at 4:6 and 10:0 ratios (121 ± 4% and 132 ± 4%, respectively, as compared with the 1:9 ratio) (Figure 2A). These data were further confirmed using a complementary approach: adeno-associated viral (AAV)-mediated overexpression of PS1 was tagged with green fluorescent protein (GFP) at the N-erminus and the red fluorescent protein (RFP) was inserted in the loop domain, and the determination of the proximity between the fluorophores was made using spectral FRET (Supplementary Figure S1). Similarly, higher FRET efficiency was recorded in the neurons pretreated with the Aβ42/40 peptides at the 4:6 and 10:0 ratios.

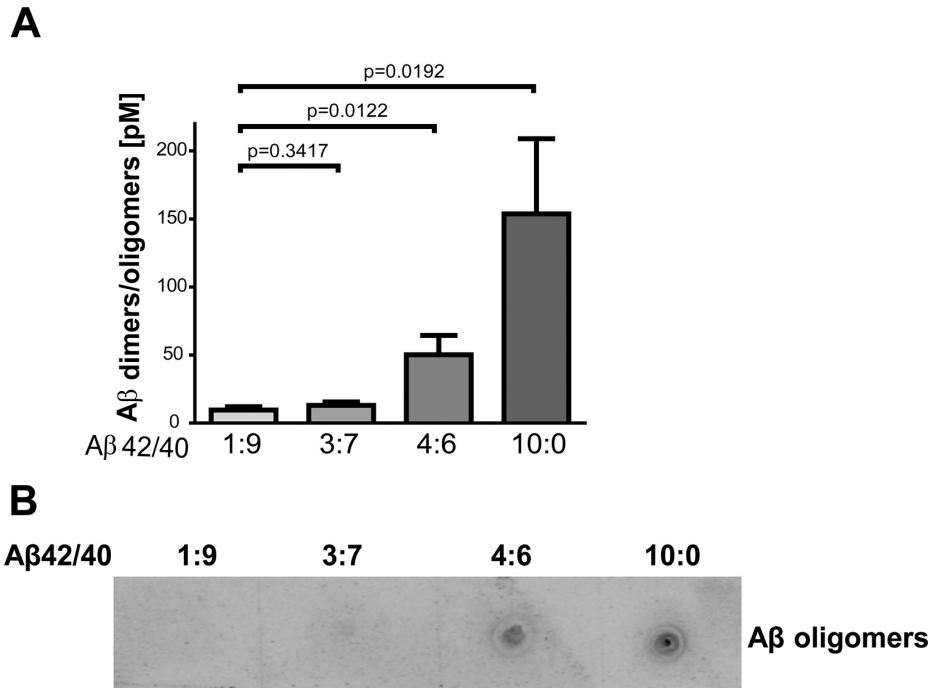

Figure 1. Characterization of Aβ peptides. (A) ELISA analysis of the Aβ dimers/oligomers in the mixtures of the Aβ42 and Aβ40 peptides mixed at the ratios of 1:9, 3:7, 4:6 and 10:0 at the total 1 μmol/L Aβ concentration. n = 9, mean ± SEM, two-tailed unpaired Student *t* test. (B) The representative dot blot presents the abundance of Aβ oligomers detected by Aβ oligomer specific antibody in the mixtures of the Aβ42 and Aβ40 peptides mixed at the ratios of 1:9, 3:7, 4:6 and 10:0 at the total 1 μmol/L Aβ concentration. Aβ – amyloid β.

These data suggest at least two possibilities: the conformational shift of PS1 toward the closed, pathogenic state may be induced either by higher Aβ42/40 ratio or by higher Aβ42 concentration. To distinguish between these two possibilities, the neurons were treated with Aβ42 and Aβ40 peptides at the following ratios and relative amounts, respectively: 1:9 (0.1 μmol/L Aβ42: 0.9 μmol/L Aβ40), 4:6 (0.4 μmol/L Aβ42: 0.6 μmol/L Aβ40), 1:0 (0.1 μmol/L Aβ42 alone) and 4:0 (0.4 μmol/L Aβ42 alone). Consistent with the previous finding, the increase in the Aβ42/40 ratio from 1:9 to 4:6 resulted in the conformational change of PS1 toward the pathogenic state. Although a trend toward more severe change in PS1 conformation was observed in the 4:0-treated cells (Aβ42:Aβ40), compared with that with the 4:6 treatment (Aβ42:Aβ40), no statistically significant difference between neurons treated with the Aβ42 to Aβ40 ratios at 4:6 versus 1:0 versus 4:0 was observed (all had "closed" PS1 conformation). Intriguingly, even though the absolute amount of Aβ42 was the same in the Aβ42:Aβ40 at the 1:9 and 1:0 conditions (0.1 μmol/L), PS1 adapted closed, pathogenic conformation only in the latter (Figure 2B). These data would support the hypothesis that the ratio of the Aβ42/40 rather than the absolute Aβ42 level is crucial for PS1 conformational change and imply that presence of the Aβ40 might decrease the pathogenic effect of the longer Aβ species on PS1 conformation.

Increased Intracellular Calcium Load Due to High Aβ42/40 Ratio Leads to Pathogenic Shift in PS1 Conformation

Next we investigated the potential mechanisms by which Aβ42 and Aβ40 peptides at the high Aβ42/40 ratio might cause the pathogenic change within the PS1 subdomain architecture. First, to exclude the possibility that the observed effect is due to neurotoxicity of the applied Aβ treatment, we monitored the level of lactate dehydrogenase in conditioned medium from the control and Aβ-treated neurons. We determined that treatments with the given Aβ concentrations, irrespective of the Aβ42/40 ratio, did not cause any significant cytotoxicity (Figure 3).

As Aβ has been linked to impaired Ca^{2+} homeostasis, we assayed calcium levels in neurons treated with the 1:9, 3:7, 4:6 or 10:0 ratios of Aβ42:Aβ40 using an Indo-1 reporter probe. Elevated intracellular calcium levels were observed only after the treatment with Aβ mixtures containing Aβ42 and Aβ40 peptides in the 4:6 and 10:0 ratios (Figure 4A). The increase in the intracellular calcium load correlated with the higher FRET efficiency between fluorescently labeled PS1 domains (Figure 4B).

To confirm that the observed effects are physiologically relevant, we conducted additional experiments where Aβ concentration was reduced to the nanomolar range. For these we chose to compare the effect of the mixtures containing Aβ42 and Aβ40 at the 1:9 and 4:6 ratios, that showed distinct Aβ-mediated effects on intracellular PS1 conformation (Figure 2) and intracellular Ca^{2+} (Figure 4A). The neurons incubated with the medium containing Aβ42 and Aβ40 at the 4 nmol/L and 6 nmol/L concentrations, respectively, (4:6 ratio) presented higher intracellular calcium levels and altered conformation of PS1 when compared with the neurons treated with the mixture of 1 nmol/L Aβ42 and 9 nmol/L Aβ40 (1:9 ratio) (Supplementary Figure S2). This supports the physiological relevance of the observed Aβ-mediated effects.

To verify the effect of calcium influx on the conformational shift of endogenous PS1, we stimulated primary neurons with 50 mmol/L KCl and assayed the proximity between fluorophores labeling the PS1 N-terminus and the PS1 loop domain using antibody-based

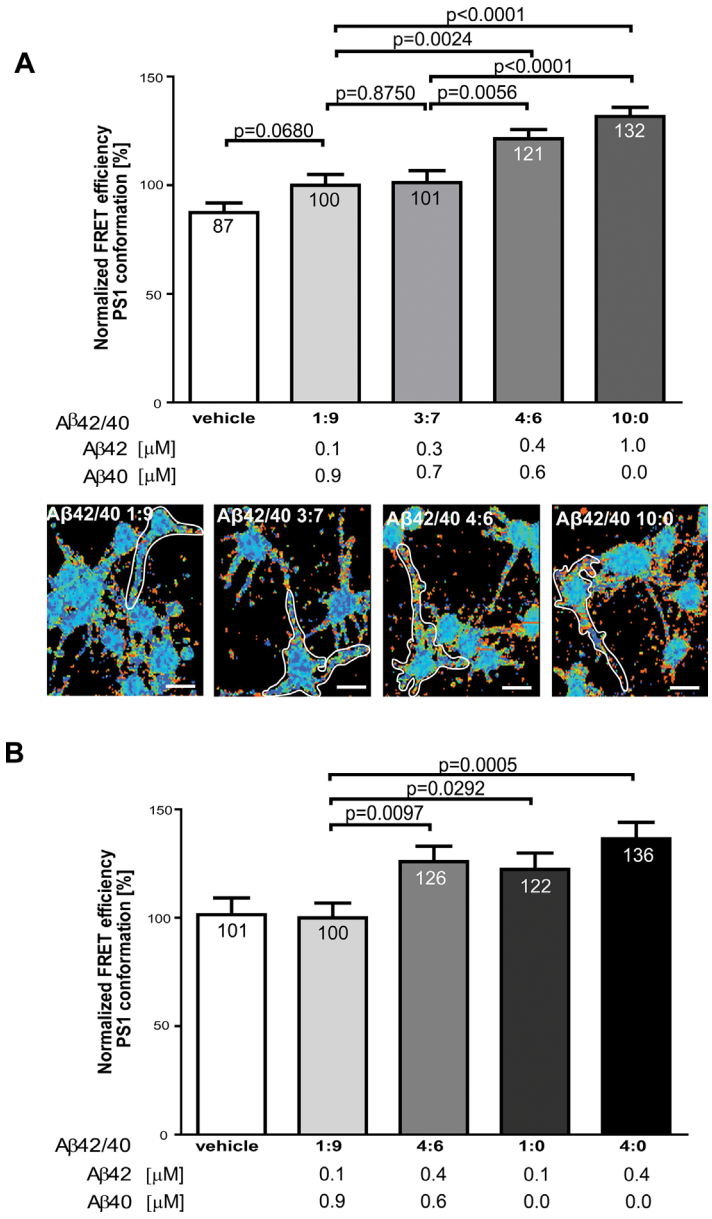

Figure 2. Effect of Aβ42/40 ratio on PS1 conformation. (A) FLIM analysis of the PS1 conformation in primary neurons pretreated for 2 h with the mixtures of Aβ42 and Aβ40 peptides at (A) the varied ratios at the 1 μmol/L total Aβ concentration or (B) the varied ratios (1:9 or 4:6) at the 1 μmol/L total Aβ concentration or different absolute amounts of Aβ42 (0.1 μmol/L or 0.4 μmol/L). The graphs present the increase in FRET efficiency, corresponding to "closed" PS1 conformation, in neurons treated with Aβ42 to Aβ40 at the relatively high ratios. (A) n = 73 (vehicle), n = 77 (1:9), n = 74 (3:7), n = 157 (4:6), n = 152 (10:0), (B) n = 50 (vehicle), n = 50 (1:9), n = 49 (4:6), n = 51 (1:0), n = 50 (4:0), n = total number of neurons analyzed from three independent experiments, mean ± SEM; two-tailed unpaired Student *t* test. The data are normalized to the values recorded in neurons pretreated with Aβ42 and Aβ40 peptides at the 1 to 9 ratio. The images present color-coded lifetime of the donor fluorophore. The red pixels correspond to the shorter donor fluorophore lifetimes, indicative of higher FRET efficiency (relative proximity) between the fluorescently labeled PS1 domains. The scale bar corresponds to 10 μm. Aβ – amyloid β; PS1 – presenilin 1; FRET – Förster resonance energy transfer.

FLIM. An increase in the intracellular calcium levels and the shift of PS1 toward the pathogenic state were recorded in KCl-treated neurons (Figures 5A, B). Importantly our previous data demonstrating an increase in the Aβ42/40 ratio upon the rise in intracellular calcium (20) support the functional relevance of the observed shift within the PS1 subdomain organization.

To further determine if the increase in the intracellular calcium load is indeed causative of the conformational shift of PS1, we applied another calcium elevating agent, A2317 calcium ionophore, to the primary neurons overexpressing G-PS1-R probe as a reporter of the PS1 conformation. Application of the A2317 resulted in a marked rise in the intracellular calcium load (Figure 5C), which corresponded to the increased FRET efficiency between the GFP and RFP labeling the respective PS1 domains, compared with the control (Figure 5D). This argues in favor of the relationship between the elevated calcium and pathogenic conformational changes within the PS1 molecule.

DISCUSSION

As PS1/γ-secretase is the enzyme responsible for the final cut of the amyloid precursor protein (APP) substrate producing Aβ peptides, altered PS1 structure and function would affect the composition of Aβ species generated. The Aβ aggregates in the brain are surrounded by significantly altered microenvironment exhibiting gliosis and an increased level of reactive oxygen species and calcium dyshomeostasis and a substantial accumulation of the soluble oligomeric Aβ in a halo enclosing the plaque core (22–25). However, the crosstalk between all these insults and PS1 architecture remains poorly understood.

The current study demonstrates that there is a reciprocal relationship between elevated Aβ42 or Aβ42/40 ratio and the pathogenic conformational state of PS1. Our data imply that an increased Aβ42/40 ratio could trigger a conformational shift of PS1 toward the

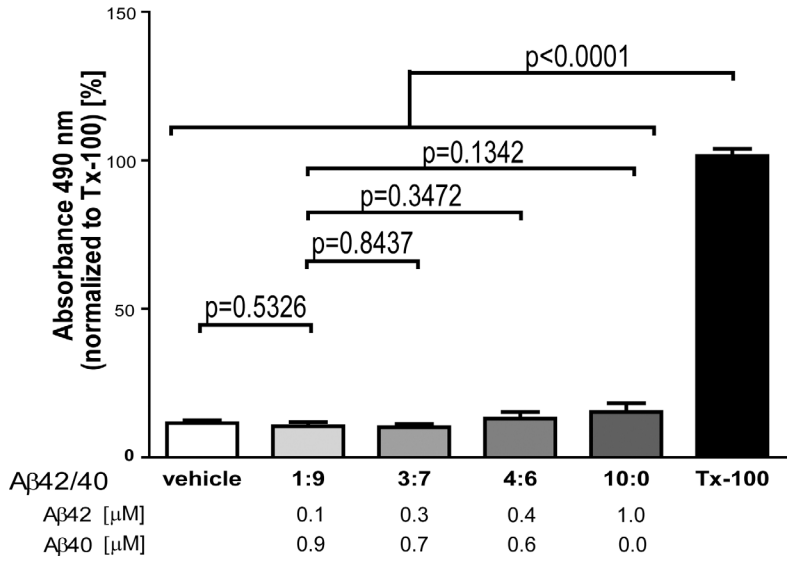

Figure 3. Cytotoxicity of Aβ treatment. Relative levels of the lactate dehydrogenase (LDH) activity in the conditioned medium after Aβ treatments. 1% Tx-100 is used as a positive control. n = 21 (vehicle), n = 18 (1:9), n = 15 (3:7), n = 18 (4:6), n = 17 (10:0), n = 18 (Tx-100), mean ± SEM, two-tailed unpaired Student *t* test. Aβ – amyloid β, Tx-100 – Triton X-100.

pathogenic state by means of increasing intracellular calcium load. This is in line with the data suggesting the importance of the Aβ42/40 ratio in the AD progression and proposing calcium dyshomeostasis as one of the culprits exacerbating AD pathology (26–28).

Impairments in intracellular calcium can serve as an insult, provoking several alterations in the neuronal functions including activation of mitochondrial stress responses (29), disruption of spinodendritic signaling interface (30) and apoptosis (31), and can also accelerate Aβ fibril formation (32). The latter would suggest an existence of a feed-forward mechanism of calcium impairments and toxic Aβ generation. Our findings point toward yet another possible mechanism spinning the vicious cycle. We propose that Aβ peptides at the elevated ratio of Aβ42 to Aβ40, which results from the pathogenically altered cleavage of the amyloid precursor protein (APP) by PS1 (8), increase the intracellular calcium load, which could in turn modulate conformation of the PS1 enzyme.

Several mechanisms can be implicated in the calcium-mediated pathogenic reorganization of PS1. One possibility is that calcium influx results in the rearrangement of the PS1-interacting partners, which triggers different degrees of "squishing" of the highly flexible PS1/γ-secretase. Alternatively, the calcium influx may induce posttranslational modifications in PS1. Such posttranslational modifications may result in the rearrangements within the PS1 subdomain architecture by altering local charges and atomic forces within the PS1 molecule.

An atomic structure of the γ-secretase complex at 3.4Å resolution has recently been reported (33). However, the precise molecular reshuffles of the PS1 domains on the atomic level caused by various factors remain unknown. Recent studies using cysteine cross-linking have demonstrated a correlation between the distance of the cytosolic residues in PS1 transmembrane domains 4 and 7 and Aβ42 generation, proposing that the dynamics of this region might be impaired by PS1 mutations (34). In addition, simulated modeling of the dynamic repositioning of the PS1 cytosolic loop suggested that it may control substrate access and cleavage precision, and these can be affected by fAD mutations (35). The PS1 conformation assay that we employ in this study detects relative changes between the cytosolic loop and PS1 N-terminus in response to Aβ in intact neurons. Although the FRET-based PS1 conformation assay applied here does not address the detailed structural rearrangements within the PS1 molecule, it can reliably distinguish between the "normal" and "pathogenic" PS1 conformations *in situ*, as determined by us and others (11,13,17,36). The relatively small changes observed in the FRET efficiency, reflecting proximity between fluorescent tags on PS1, may translate into much greater alterations in PS1 on the sub-molecular scale. It is highly likely that even small changes that persist over a long time may have a detrimental effect.

Our findings also indicate that Aβ40 may decrease the pathogenic effect of Aβ42 on PS1 conformation, suggesting that it could serve as a protective factor under a certain threshold of Aβ42. We found that adding 0.9 μmol/L Aβ40 to the media containing 0.1 μmol/L Aβ42 prevented the Aβ42-induced pathogenic PS1 conformational change, even though the total Aβ concentration in this case was ~10 times higher than in 0.1 μmol/L Aβ42 alone (Figure 2B). The potential protective effect of Aβ40, however, has limits, and 0.6 μmol/L Aβ40 no longer averts the detrimental effect of 0.4 μmol/L Aβ42 on PS1 conformation (4:6 versus 4:0 Aβ42/40 ratio). These data are in agreement with the previous reports suggesting a protective role of the Aβ40 by showing that Aβ40 could rescue Aβ42-induced cell death *in vitro* (10,37). The prevention of Aβ42 aggregation and toxicity was proposed as a possible mechanism of the Aβ40 effect. Together, these data support the idea that a reduced level of Aβ40 and/or an increased Aβ42/40 ratio in the brain, rather than the absolute Aβ amount, may be detrimental factors in AD.

Importantly, our current findings suggest that Aβ may trigger PS1

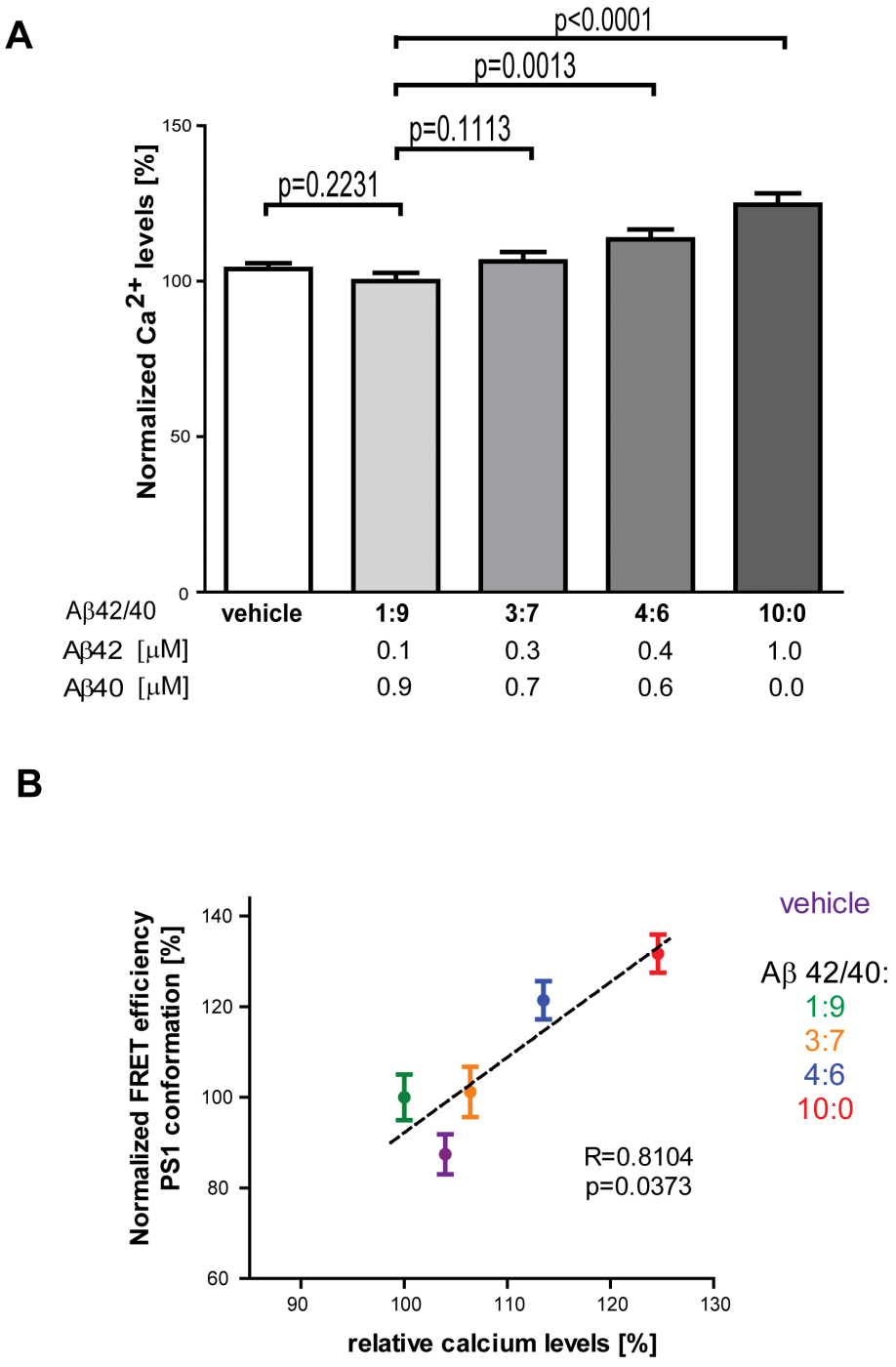

Figure 4. Intracellular calcium level upon Aβ treatment. (A) The relative levels of intracellular calcium in primary neurons were determined using ratiometric Indo-1 dye. The graph presents the increase in the calcium level upon treatment with Aβ peptides at increasing Aβ42/40 ratio. n = 234 (vehicle), n = 243 (1:9), n = 271 (3:7), n = 263 (4:6), n = 219 (10:0), n = total number of neurons analyzed from three independent experiments, mean ± SEM, two-tailed unpaired Student *t* test. (B) Correlation between PS1 conformational changes (FRET efficiency) and intracellular calcium levels in primary neurons treated with vehicle or Aβ42 to Aβ40 at 1:9; 3:7; 4:6 or 10:0 ratios. Pearson's X-square test. Aβ – amyloid β; PS1 – presenilin 1; FRET – Förster resonance energy transfer.

conformational change associated with increased Aβ42 production in the neighboring neurons, which would exacerbate and possibly incite propagation of the amyloid pathology. Although the observed alterations triggered by the relatively short (2 h) Aβ pretreatment in the reported experimental settings are comparatively small, the prolonged exposure to the pathogenic perturbations would result in the progressive development of the pathology.

In summary, our findings link three key players in AD pathogenesis, toxic Aβ42 specie, PS1/γ-secretase and impairments in calcium homeostasis, provide novel insight into the progressive exacerbation of AD pathology, and point toward molecular events which might be targeted for therapeutic intervention.

CONCLUSION

Our findings demonstrate that extracellular amyloid β (Aβ) peptides, when present at a relatively high ratio of the longer to shorter (Aβ42 to Aβ40) species, trigger an increase in the intracellular calcium level in the affected neuron. This leads to a pathogenic conformational shift in the endogenous PS1/γ-secretase within the cell, favoring further production of the longer Aβ peptides, and results in an increased ratio of Aβ42 to Aβ40. These events can occur reciprocally in Aβ-producing cells as well as in the neighboring neurons, demonstrating a noncell autonomous mechanism of Aβ action. The discovery of the novel mechanism of potential exacerbation of the amyloid pathology may facilitate the design of new therapeutic approaches focused on inhibition of the disease progression by "stabilizing" PS1 conformation.

ACKNOWLEDGMENTS

We thank Shuko Takeda for guidance with preparation of the Aβ peptides and Sarah Svirsky for help with primary neuronal cultures. The work was supported by NIH grants AG 044486 and AG 15379 (OB).

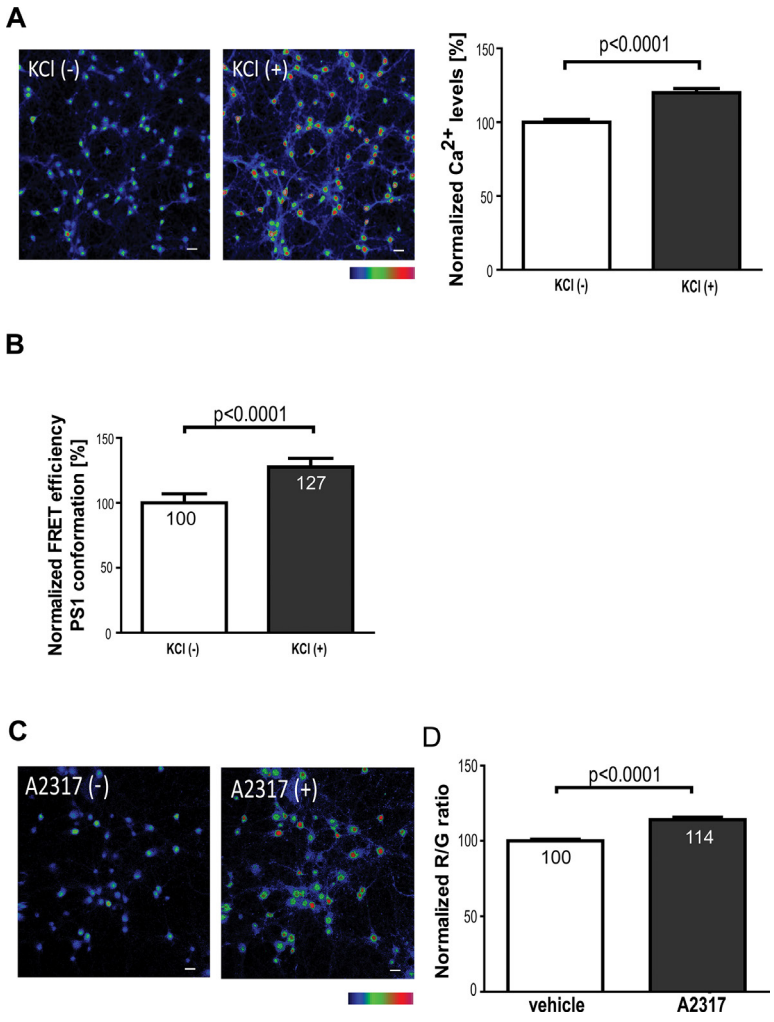

Figure 5. Ca^{2+} overload triggers conformational change of PS1. (A) Increase in the intracellular calcium levels in neurons treated with 50 mmol/L KCl is monitored by Oregon Green BAPTA-1/AM (images) or by Indo-1 ratiometric probe (graph). The pseudo-colored images show intracellular calcium levels pre- and post-treatment. The red pixels correspond to higher calcium levels. The graph presents quantification of the intracellular calcium levels. n = 310 (KCl–) n = 251 (KCl+), n = total number of neurons analyzed from three independent experiments mean ± SEM, two-tailed unpaired Student *t* test. The scale bar corresponds to 20 μm. (B) FLIM analysis of the PS1 conformation pre- and post-KCl treatment in neurons. Increase in the FRET efficiency, reflective of pathogenic "closed" PS1 conformation, is detected after 15 min of KCl treatment. n = 84 (KCl–) n = 85 (KCl+), n = total number of neurons analyzed from 3 independent experiments, mean ± SEM, two-tailed unpaired Student *t* test. The data are normalized to the values recorded in the neurons in KCl– conditions. (C) Increase in the intracellular calcium levels in neurons treated with 5 μmol/L A2317 calcium ionophore monitored by Oregon Green BAPTA-1/AM. The pseudo-colored images show intracellular calcium levels pre- and post-treatment. The red pixels correspond to higher calcium levels. The scale bar corresponds to 20 μm. (D) Spectral FRET analysis of the PS1 conformation pre- and post-A2317 calcium ionophore treatment in primary neurons. Increase in FRET efficiency (R/G ratio) reflective of pathogenic "closed" PS1 conformation is detected in A2317-treated neurons. n = 180 (vehicle) n = 185 (A2317), n = total number of neurons analyzed from three independent experiments, mean ± SEM, two-tailed unpaired Student *t* test. Aβ – amyloid β; PS1 – presenilin 1; FRET – Förster resonance energy transfer.

DISCLOSURE

The authors declare they have no competing interests as defined by *Molecular Medicine*, or other interests that might be perceived to influence the results and discussion reported in this paper.

REFERENCES

1. Hardy J, Selkoe DJ. (2002) The amyloid hypothesis of Alzheimer's disease: progress and problems on the road to therapeutics. *Science*. 297:353–6.
2. Braak H, Braak E, Ohm T, Bohl J. (1989) Alzheimer's disease: mismatch between amyloid plaques and neuritic plaques. *Neurosci. Lett*. 103:24–28.
3. Takami M, *et al*. (2009) gamma-Secretase: successive tripeptide and tetrapeptide release from the transmembrane domain of beta-carboxyl terminal fragment. *J. Neurosci*. 29:13042–52.
4. Roychaudhuri R, *et al*. (2013) C-terminal turn stability determines assembly differences between Abeta40 and Abeta42. *J. Mol. Biol*. 425:292–308.
5. Ran Y, *et al*. (2014) gamma-Secretase processing and effects of gamma-secretase inhibitors and modulators on long Abeta peptides in cells. *J. Biol. Chem*. 289:3276–87.
6. Chen YR, Glabe CG. (2006) Distinct early folding and aggregation properties of Alzheimer amyloid-beta peptides Abeta40 and Abeta42: stable trimer or tetramer formation by Abeta42. *J. Biol. Chem*. 281:24414–22.
7. Klein AM, Kowall NW, Ferrante RJ. (1999) Neurotoxicity and oxidative damage of beta amyloid 1–42 versus beta amyloid 1–40 in the mouse cerebral cortex. *Ann. N. Y. Acad. Sci*. 893:314–20.
8. Fernandez MA, Klutkowski JA, Freret T, Wolfe MS. (2014) Alzheimer presenilin-1 mutations dramatically reduce trimming of long amyloid beta-peptides (Abeta) by gamma-secretase to increase 42-to-40-residue Abeta. *J. Biol. Chem*. 289:31043–52.
9. Kuperstein I, *et al*. (2010) Neurotoxicity of Alzheimer's disease Abeta peptides is induced by small changes in the Abeta42 to Abeta40 ratio. *EMBO J*. 29:3408–20.
10. Jan A, Gokce O, Luthi-Carter R, Lashuel HA. (2008) The ratio of monomeric to aggregated forms of Abeta40 and Abeta42 is an important determinant of amyloid-beta aggregation, fibrillogenesis, and toxicity. *J. Biol. Chem*. 283:28176–89.
11. Uemura K, *et al*. (2009) Allosteric modulation of PS1/gamma-secretase conformation correlates with amyloid beta(42/40) ratio. *PloS One*. 4:e7893.
12. Elad N, *et al*. (2015) The dynamic conformational landscape of gamma-secretase Nadav. *J. Cell Science*. 128:589–98.
13. Berezovska O, *et al*. (2005) Familial Alzheimer's disease presenilin 1 mutations cause alterations in the conformation of presenilin and interactions with amyloid precursor protein. *J. Neurosci*. 25:3009–17.

14. Ingelsson M, *et al*. (2004) Early Abeta accumulation and progressive synaptic loss, gliosis, and tangle formation in AD brain. *Neurology*. 62:925–31.
15. Wahlster L, *et al*. (2013) Presenilin-1 adopts pathogenic conformation in normal aging and in sporadic Alzheimer's disease. *Acta Neuropathol*. 125:187–99.
16. Placanica L, Zhu L, Li YM. (2009) Gender- and age-dependent gamma-secretase activity in mouse brain and its implication in sporadic Alzheimer disease. *PloS One* 4:e5088.
17. Lleo A, *et al*. (2004) Nonsteroidal anti-inflammatory drugs lower Abeta42 and change presenilin 1 conformation. *Nat. Med*. 10:1065–6.
18. Ohki Y, *et al*. (2011) Phenylpiperidine-type gamma-secretase modulators target the transmembrane domain 1 of presenilin 1. *EMBO J*. 30:4815–24.
19. Takeda S, *et al*. (2013) Brain interstitial oligomeric amyloid beta increases with age and is resistant to clearance from brain in a mouse model of Alzheimer's disease. *FASEB J*. 27:3239–48.
20. Kuzuya A, *et al*. (2016) Identification of the novel activity-driven interaction between synaptotagmin 1 and presenilin 1 links calcium, synapse, and amyloid beta. *BMC Biol*. 14:25.
21. Wu HY, *et al*. (2012) Distinct dendritic spine and nuclear phases of calcineurin activation after exposure to amyloid-beta revealed by a novel fluorescence resonance energy transfer assay. *J. Neurosci*. 32:5298–309.
22. Kuchibhotla KV, Lattarulo CR, Hyman BT, Bacskai BJ. (2009) Synchronous hyperactivity and intercellular calcium waves in astrocytes in Alzheimer mice. *Science*. 323:1211–5.
23. Xie H, *et al*. (2013) Mitochondrial alterations near amyloid plaques in an Alzheimer's disease mouse model. *J. Neurosci*. 33:17042–51.
24. Koffie RM, *et al*. (2009) Oligomeric amyloid beta associates with postsynaptic densities and correlates with excitatory synapse loss near senile plaques. *Proc. Natl. Acad. Sci. U. S. A*. 106:4012–7.
25. Osborn LM, Kamphuis W, Wadman WJ, Hol EM. (2016) Astrogliosis: An integral player in the pathogenesis of Alzheimer's disease. *Prog. Neurobiol*.. [Epub ahead of print].
26. Green KN. (2009) Calcium in the initiation, progression and as an effector of Alzheimer's disease pathology. *J. Cell. Mol. Med*. 13:2787–99.
27. Demuro A, Parker I, Stutzmann GE. (2010) Calcium signaling and amyloid toxicity in Alzheimer disease. *J. Biol. Chem*. 285:12463–8.
28. Bezprozvanny I. (2009) Calcium signaling and neurodegenerative diseases. *Trends Mol. Med*. 15:89–100.
29. Votyakova TV, Reynolds IJ. (2005) Ca2+-induced permeabilization promotes free radical release from rat brain mitochondria with partially inhibited complex I. *J. Neurochem*. 93:526–37.
30. Kuchibhotla KV, *et al*. (2008) Abeta plaques lead to aberrant regulation of calcium homeostasis in vivo resulting in structural and functional disruption of neuronal networks. *Neuron*. 59:214–25.
31. Takei N, Endo Y. (1994) Ca2+ ionophore-induced apoptosis on cultured embryonic rat cortical neurons. *Brain Res*. 652:65–70.
32. Isaacs AM, Senn DB, Yuan M, Shine JP, Yankner BA. (2006) Acceleration of amyloid beta-peptide aggregation by physiological concentrations of calcium. *J. Biol. Chem*. 281:27916–23.
33. Bai XC, *et al*. (2015) An atomic structure of human gamma-secretase. *Nature*. 525:212–7.
34. Tominaga A, Cai T, Takagi-Niidome S, Iwatsubo T, Tomita T. (2016) Conformational changes in transmembrane domain 4 of presenilin 1 are associated with altered amyloid-beta 42 production. *J. Neurosci*. 36:1362–72.
35. Somavarapu AK, Kepp KP. (2016) The dynamic mechanism of presenilin-1 function: Sensitive gate dynamics and loop unplugging control protein access. *Neurobiol. Dis*. 89:147–56.
36. Wang X, *et al*. (2015) gamma-Secretase Modulators and Inhibitors Induce Different Conformational Changes of Presenilin 1 Revealed by FLIM and FRET. *J. Alzheimers Dis*. 47:927–37.
37. Zou K, *et al*. (2003) *Amyloid* beta-protein (Abeta)1–40 protects neurons from damage induced by Abeta1–42 in culture and in rat brain. *J. Neurochem*. 87:609–19.

Cite this article as: Zoltowska KM, Maesako M, Berezovska O. (2016) Interrelationship between changes in the amyloid β 42/40 ratio and presenilin 1 conformation. *Mol. Med*. 22:329–37.